Materials Today Communications 52 (2026) 114935

Contents lists available at ScienceDirect

Materials Today Communications

journal homepage: www.elsevier.com/locate/mtcomm

# Variable order fractional model for describing the mechanical behaviour of amorphous polymers

Lin Sun [a,b], Gang Cheng [b,*], Thierry Barrière [a]

[a] Institut FEMTO-ST, National Centre for Scientific Research (CNRS), Université Marie et Louis Pasteur, Besançon 25000, France
[b] INSA Centre Val de Loire, Laboratory of Mechanics Gabriel Lamé (LaMé), Blois 41034, France

ARTICLE INFO

*Keywords:*
Glass transition temperature
Polycarbonate
Variable order fractional model
Viscoelastic behaviour

ABSTRACT

Amorphous polymers exhibit strongly temperature-dependent mechanical behaviour, particularly near the glass transition temperature, which remains challenging to describe using conventional viscoelastic models. In this study, an improved variable order fractional constitutive model is proposed to describe the viscoelastic behaviour of amorphous polymers under different temperatures. The novelty of the research lies in introducing the multiple functions for the evolution of the fractional order, enabling an accurate description of nonlinear stress-strain behaviour over a wide temperature range. Compression tests on polycarbonate are performed across temperatures spanning the glass transition, and model parameters are identified based on the experimental data. Comparisons with existing fractional order models demonstrate that the proposed model achieves accurate fitting results with fewer parameters, particularly near yielding and at large deformations. The research confirms the efficiency of the proposed variable order fractional model for describing the viscoelastic behaviour from glassy to rubbery state.

## 1. Introduction

Amorphous polymers exhibit distinct mechanical and thermal properties due to their disordered molecular structure and the absence of long-range crystalline order. The absence of a well-defined crystalline phase results in various viscoelastic behaviours [1], which is strongly influenced by temperature and strain rate. Polycarbonate (PC) is an amorphous polymer widely used in engineering applications due to its high impact resistance, transparency, toughness, and excellent mechanical stability [2–4]. Its viscoelastic behaviour is highly sensitive to temperature, especially below and above the glass transition temperature (Tg) [5]. The accurate identification of the temperature-dependent behaviours within a constitutive framework remains a significant challenge and necessitates the development of efficient models [6].

Various constitutive models have been proposed to describe the mechanical behaviour of PC over different temperatures and strain rates. Luo et al. [7] employed a linear viscoelastic formulation using multiple springs and dashpots to represent molecular elongation and slippage, successfully describing delayed elastic responses. Alves et al. [8,9] proposed a nonlinear, rate-dependent constitutive model to describe compressive behaviour below Tg, including yield and post-yield responses. These conventional viscoelastic models require a large number of parameters and are insufficient to represent consistently the material behaviour across Tg.

Fractional order models have emerged as powerful constitutive behaviour laws to conventional viscoelastic models, owing to their ability to interpolate naturally between elastic and viscous responses with fewer parameters [10,11]. These models are able to describe time-dependent and strain rate-sensitive behaviours of polymers. The fractional derivatives have been proposed to describe viscoelastic and viscoplastic responses in polymeric materials with fractal dashpots [12,13]. Salazar-Martín et al. [14] applied a fractional Voigt-Maxwell model to describe creep behaviour, showing improved fitting accuracy with fewer parameters compared to conventional models. The fractional Maxwell model provides a favourable compromise between relative simplicity and a well-established capability to accurately describe stress relaxation behaviour. The fractional Kelvin-Voigt model is more naturally suited for modelling creep responses, while the fractional Burgers model, owing to its larger number of elements and parameters, is particularly effective in describing highly nonlinear and multistage viscoelastic responses.

Constant order fractional (COF) models remain limited in describing

* Corresponding author.
*E-mail address:* gang.cheng@insa-cvl.fr (G. Cheng).

https://doi.org/10.1016/j.mtcomm.2026.114935
Received 22 October 2025; Received in revised form 26 February 2026; Accepted 27 February 2026
Available online 28 February 2026

the evolving mechanical response of polymers over large deformation ranges and across wide temperature domains. A fixed fractional order cannot describe the memory effects on the thermo-mechanical behaviours associated with the evolution of deformation. Variable order fractional (VOF) models have been introduced, allowing the fractional order to evolve as a function of deformation or time [15]. This framework enables a more flexible representation of material memory effects and evolving viscoelastic mechanisms [16]. VOF models have been applied to various materials and the fractional order could be considered as an index to identify the flow behaviour [17]. The VOF model was employed to describe the multistage compressive responses of polymer foams in the uniaxial compression tests, including the viscoelastic, softening, plateau, and densification regions [18]. Gao et al. [19] compared the VOF and COF models to describe the compressive behaviour of soft materials and demonstrated the improved fitting accuracy of VOF models.

VOF viscoelastic models have been employed to describe the stress-strain behaviour of polymeric materials. A linear variation of the fractional order with strain was employed to describe the viscoelastic response of amorphous polymers [20]. It is insufficient to describe the nonlinear mechanical response exhibited by glassy polymers [21]. The fractional order has been extended to power-law formulation to better describe their nonlinearity [22]. Variable order functions inspired by growth-curve theories have been proposed to describe strain-softening behaviour, particularly in regimes associated with logarithmic growth characteristics [23]. Cai et al. [24] proposed a VOF framework incorporating power-law fractional order functions and demonstrated that these formulations were more sensitive to temperature and more effective in describing nonlinear phenomena such as strain hardening. However, the influence of different fractional order evolution functions on modelling efficiency and predictive capability has not yet been systematically investigated.

In this study, the experimental and numerical analyses are conducted to investigate the compressive mechanical behaviour of PC over a wide temperature range across Tg. A VOF modelling framework is proposed with different fractional order functions selected according to the yield point. A linear strain-dependent order function is employed to describe the mechanical response above Tg, while below Tg, linear and power-law order functions are employed to characterize the complex strain-softening and strain-hardening behaviours. The proposed VOF models have been compared with the existing models in describing the various stress-strain curves below and above Tg. The VOF models demonstrated better agreement with experimental data and less fitting parameters.

This paper is organized into five sections. Following the Introduction, Section 2 describes the material preparation, experimental procedures, and constitutive modelling framework. Section 3 presents the parameter identification results and comparative numerical analyses. Section 4 is devoted to discussion and model assessment. The conclusions and perspectives for future work are summarized in Section 5.

## 2. Material and methods

The thermo-mechanical properties of PC were investigated based on the experimental results obtained from the thermal and mechanical tests. The PC pellets were dried to remove moisture and then injected into a cylindrical mould to fabricate the specimens for the compression tests. Differential Scanning Calorimetry (DSC) was performed to characterize the thermal properties. Uniaxial compression tests were conducted over a wide range of temperatures to evaluate the temperature-dependent viscoelastic properties under large deformations. A VOF model, in which the fractional order evolved with the deformation history, was employed to describe the observed viscoelastic behaviour. The model parameters were identified using the least squares method (LSM).

### 2.1. Material preparation

The PC INFINO® material was selected because of its good mechanical property (superior flowability and thermal stability) and outstanding optical clarity. It is suitable for a wide variety of applications from small to large size products with complex designs. As illustrated in the manufacturing process shown in Fig. 1, the PC pellets were dried in a thermal oven at 120 °C for 4 h to remove residual moisture before injection moulding, ensuring consistent processing conditions. It was carried out with a screw of 15 mm, maximum injection pressure of 220 MPa and maximum injection volume of 12 $cm^3$. The polymer injection temperature was set to 300 °C, while the mould temperature was set to 90 °C. These processing parameters were selected based on the material specifications and preliminary optimization trials to ensure dimensional accuracy in the moulded specimens. After injection, the final specimens were obtained by turning process, with a diameter of 10 mm and a length of 10 mm.

DSC tests were performed to characterize the thermal behaviour of PC. The evolution of heat flow was measured using a specimen with a mass of 28.0 mg, placed in an aluminium crucible and subjected to a controlled heating programme. The heating rate was set to 2 °C/min in order to ensure adequate sensitivity while minimizing thermal lag during the measurement. A lower heating rate improves the resolution of overlapping thermal events and reduces the potential shift of transition temperatures associated with kinetic effects [25]. The temperature range was selected from 25 to 300 °C to encompass all relevant thermal transitions of PC, including Tg, as well as possible endothermic or degradation phenomena at higher temperatures. Following the heating stage, the sample was cooled to 25 °C to complete the thermal cycle.

Fig. 2 presents the DSC thermogram illustrating the evolution of heat flow as a function of temperature. Tg is identified from the characteristic step change in the baseline of the heat flow signal, which reflects an increase in heat capacity associated with the transition from the glassy to rubbery state. Tg is defined as the temperature corresponding to the midpoint of the heat capacity change between the extrapolated baselines of the glassy and rubbery regions. The value of Tg is estimated to be approximately 143 °C. It is consistent with reported literature data for PC and confirms the occurrence of the glass transition within the investigated temperature range.

### 2.2. Mechanical tests

The uniaxial compression tests were performed to study its thermo-rheological properties in the temperature range from 60 to 180 °C. They were carried out at a constant strain rate on an Instron universal testing machine in accordance with the ISO 604 standard. This machine provided quasi-static loading conditions and was equipped with a thermal oven covering the range from 20 to 300 °C. A strain rate 0.003 $s^{-1}$ was applied and the true strain reached more than 50%.

The specimen shown in Fig. 3 was positioned between the upper and lower platens of a thermal oven. It was preheated to the testing temperature and maintained for 20 min to ensure uniform thermal distribution within the specimen. During the compression test, the applied force and the corresponding axial displacement were continuously recorded by the load cell and the displacement sensor.

### 2.3. Based on the measured deformation data, the true strain $\varepsilon(t)$ is calculated as follows

$$\varepsilon(t) = \ln\left(\frac{l_0}{l}\right) \tag{1}$$

where $l_0$ and $l$ are the initial and final heights of the specimen. The true stress $\sigma(t)$ is obtained as follows:


**Fig. 1.** Manufacturing process of cylindrical PC specimens.

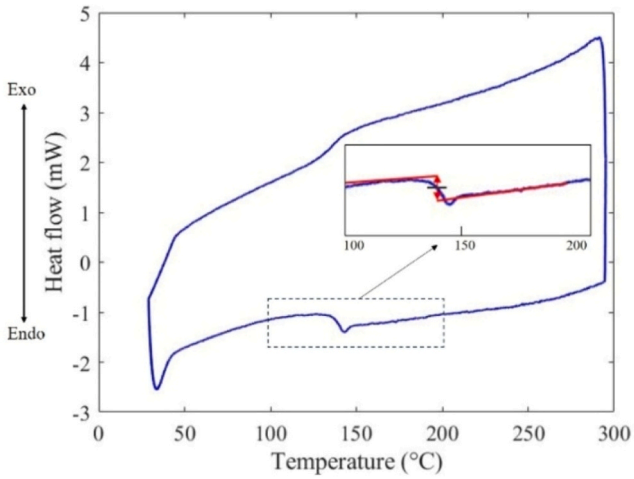


**Fig. 2.** DSC heat flow curve of PC for Tg identification.

$$\sigma(t) = \frac{Fl}{S_0 l_0} \tag{2}$$

where $S_0$ is the initial cross-sectional area of the specimen and $F$ denotes the applied force. Other symbols are explained in Table 1.

### 2.4. VOF constitutive model

A fractional derivative-based model has been proposed to describe the nonlinear properties of amorphous polymers, particularly their viscoelastic behaviour [26]. Fractional calculus extends the conventional differentiation to non-integer orders, providing an efficient representation of the gradual transition between elastic and viscous behaviour [27]. The constitutive relation of the COF model is expressed as [28]:

$$\sigma(t) = E\theta^{\alpha} D_t^{\alpha}\varepsilon(t), \quad 0 < \alpha < 1 \tag{3}$$

where $E$ is elastic modulus, $\theta = \eta/E$ is relaxation time, $\eta$ is viscosity, $D_t^{\alpha}\varepsilon(t)$ represents the fractional derivative of order $\alpha$ of true strain.

The fractional order could be appropriately adjusted as an explicit function of time, $\alpha(t)$, to enhance the predictive accuracy of fractional order models. The VOF model with $\alpha(t)$ is proposed to more effectively describe the time-dependent evolution of material response. The corresponding stress-strain relationship is expressed as follows [16]:

$$\sigma(t) = E\theta^{\alpha(t)} D_t^{\alpha(t)}\varepsilon(t), \quad 0 < \alpha(t) < 1 \tag{4}$$

where $D_t^{\alpha(t)}\varepsilon(t)$ represents the VOF derivative of $\varepsilon(t)$, $\alpha(t)$ represents the time-dependent fractional order.

The definition of VOF derivative is proposed by Ramirez and Coimbra [16]. The true strain of polymers is treated as a continuous function of time, the VOF differential operator is simplified to the Caputo form:

$$D_t^{\alpha(t)}\varepsilon(t) = \frac{1}{\Gamma(1-\alpha(t))}\int_0^t (t-s)^{-\alpha(t)} D_s^1\varepsilon(s)ds \tag{5}$$

where $\Gamma(\chi) = \int_0^{\chi} e^{-s}s^{\chi-1}ds$ is a Gamma function. $D_s^1\varepsilon(s)ds$represents the first derivative of $\varepsilon(s)$ with respect to variable $s$.

When the strain rate is constant, the true strain $\varepsilon(t)$ is defined by the following expression:

$$\varepsilon(t) = \dot{\varepsilon}t \tag{6}$$

where $\dot{\varepsilon}$ denotes the constant strain rate. The fractional order is defined as a function of strain $\alpha(\varepsilon)$ in this study, to characterize the viscoelastic behaviour as the deformation evolves.

According to the definition in Eq. (5) and Eq. (6), the VOF differential operator of $\varepsilon(t)$ is rewritten as:

$$D^{\alpha(\varepsilon)}\varepsilon(t) = \frac{1}{\Gamma(1-\alpha(\varepsilon))}\int_0^t (t-s)^{-\alpha(\varepsilon)}\dot{\varepsilon}ds = \frac{\dot{\varepsilon}}{\Gamma(1-\alpha(\varepsilon))}\bullet\frac{t^{1-\alpha(\varepsilon)}}{1-\alpha(\varepsilon)} \tag{7}$$

The Gamma function has the following property

$$\Gamma(x+1) = x\Gamma(x) \tag{8}$$

Based on the property of Gamma function, Eq. (7) is transformed as:

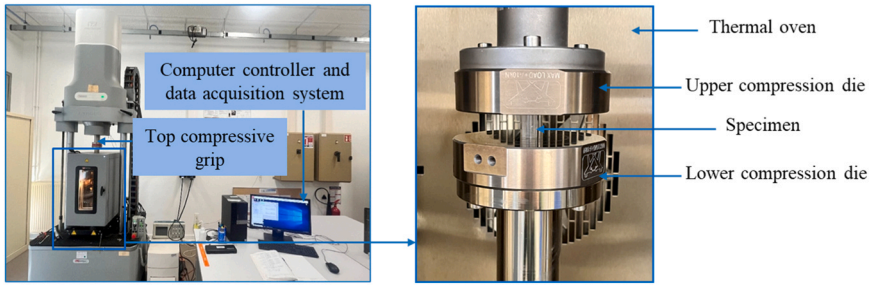


**Fig. 3.** Compression test with cylindrical PC specimen in different temperatures and strain rates.

**Table 1**
Definition of the symbols and their units.

| Parameter | Symbol | Unit |
|---|---|---|
| True strain | $\varepsilon(t)$ | – |
| True stress | $\sigma(t)$ | MPa |
| Initial height of the specimen | $l_0$ | mm |
| Final height of the specimen | $l$ | mm |
| Initial cross-sectional area of the specimen | $S_0$ | $mm^2$ |
| Force | $F$ | N |
| Constant fractional order | $\alpha$ | – |
| Time-dependent fractional order | $\alpha(t)$ | – |
| Strain-dependent fractional order | $\alpha(\varepsilon)$ | – |
| Elastic modulus | $E$ | MPa |
| Elastic modulus before yielding | $E_1$ | MPa |
| Elastic modulus after yielding | $E_2$ | MPa |
| Relaxation time | $\theta$ | s |
| Relaxation time before yielding | $\theta_1$ | s |
| Relaxation time after yielding | $\theta_2$ | s |
| Viscosity | $\eta$ | MPa·s |
| Fractional derivative | $D_t^{\alpha}(\bullet)$ | $s^{-\alpha}$ |
| Variable order fractional derivative | $D_t^{\alpha(t)}(\bullet)$ | $s^{-\alpha(t)}$ |
| Gamma function | $\Gamma(\bullet)$ | – |
| Strain rate | $\dot{\varepsilon}$ | $s^{-1}$ |
| Time | $t$ | s |
| Experimental stress | $\sigma_i(\varepsilon_i)$ | MPa |
| Predicted stress | $\widehat{\sigma}_i(\varepsilon_i, X)$ | MPa |
| Mean of stresses | $\overline{\sigma}$ | MPa |
| Number of experimental data points | $n$ | – |
| Fractional order below Tg | $\alpha_1(\varepsilon)$ | – |
| Fractional order above Tg | $\alpha_2(\varepsilon)$ | – |
| Linear slope below Tg | $a_1$ | – |
| Linear slope above Tg | $a_2$ | – |
| Intercept above Tg | $b_2$ | – |
| Scaling parameter | $c$ | – |
| Exponent | $d$ | – |
| Offset | $e$ | – |
| Pre-yield strain | $\varepsilon_1$ | – |
| Post-yield strain | $\varepsilon_2$ | – |
| Upper yield strain | $\varepsilon_Y$ | – |
| Lower yield strain | $\varepsilon_Y$ | – |
| Mechanical dissipation rate | $\mathscr{D}(t)$ | $W\bullet m^{-3}$ |
| Helmholtz free-energy density | $\psi(t)$ | $J\bullet m^{-3}$ |
| Complex modulus | $E^*(\omega, \varepsilon)$ | MPa |
| Storage modulus | $E'(\omega, \varepsilon)$ | MPa |
| Loss modulus | $E''(\omega, \varepsilon)$ | MPa |
| Angular frequency | $\omega$ | $rad\bullet s^{-1}$ |
| Imaginary unit | $i$ | – |
| Laplace variable | $s$ | $s^{-1}$ |
| Laplace transform | $F(s)$ | – |
| Real part of complex variable | $\mathrm{Re}(s)$ | – |

$$D^{\alpha(\varepsilon)}\varepsilon(t) = \frac{\dot{\varepsilon}t^{1-\alpha(\varepsilon)}}{\Gamma(2-\alpha(\varepsilon))} \tag{9}$$

The relationship between stress and strain is written as following:

$$\sigma(t) = E(\dot{\varepsilon}\theta)^{\alpha(\varepsilon)}\frac{\varepsilon(t)^{1-\alpha(\varepsilon)}}{\Gamma(2-\alpha(\varepsilon))} \tag{10}$$

### 2.5. Model parameter identification process

The parameters in the VOF model (Eq. (10)) were identified based on experimental data using LSM. The main idea of the method is to determine the model parameters, including the fractional order, by minimizing the discrepancy between experimental data and model predictions:

$$\min_X \sum_{i=1}^{N} [\sigma_i(\varepsilon_i) - \widehat{\sigma}(\varepsilon_i, X)]^2 \tag{11}$$

where $X = \{\alpha(\varepsilon), E, \theta\}$ denotes the vector of model parameters to be identified, $\sigma_i(\varepsilon_i)$ represents the experimental stress measured at the strain $\varepsilon_i$, and $\widehat{\sigma}_i(\varepsilon_i, X)$ is the corresponding stress predicted by the VOF model. The model parameters are fitted and optimized by minimizing the total squared error between experimental measurements and model predictions.

The accuracy of the parameter identification was evaluated using the root mean square error (RMSE) and the coefficient of determination ($R^2$), defined as follows:

$$\mathrm{RMSE} = \sqrt{\frac{1}{n}\sum_{i=1}^{n}(\sigma_i - \widehat{\sigma}_i)^2} \tag{12}$$

$$R^2 = 1 - \frac{\sum_{i=1}^{n}(\sigma_i - \widehat{\sigma}_i)^2}{\sum_{i=1}^{n}(\sigma_i - \overline{\sigma})^2} \tag{13}$$

where $\overline{\sigma}$ is the mean of the true stress values, $n$ is the number of experimental data points.

RMSE quantifies the absolute error between the predicted and experimental values. A lower RMSE indicates greater predictive accuracy for individual data points. $R^2$ measures the proportion of variance explained by the proposed model for the overall trend in the data. A higher $R^2$ (closer to 1) reflects a stronger fit, meaning a better capability of the model to account for the variability in the experimental data.

The flowchart of the parameter identification method is presented in Fig. 4. The mechanical behaviour of PC below and above Tg exhibits distinct characteristics, requiring different types of fractional order functions to accurately describe the material behaviours. The appropriate fractional order functions based on the yield strain are investigated in the following section.

## 3. Parameter identification and numerical analysis

This section presents an analysis of the mechanical behaviour of PC under uniaxial compression tests over a wide temperature range. The evolution of true stress-strain responses is studied at different temperatures to quantify the viscoelasticity of the material. The experimental data were obtained by conducting compression tests below and above

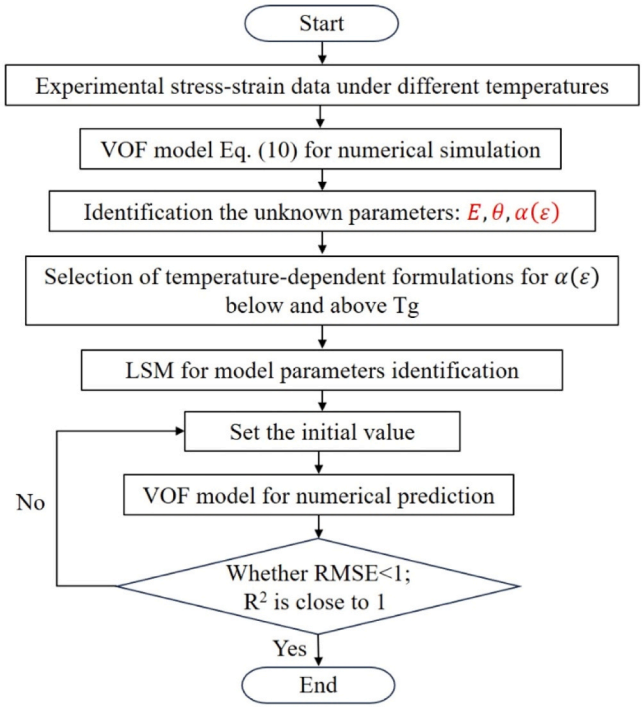


**Fig. 4.** Flowchart of parameter identification procedure for the VOF model.

Tg. The proposed VOF model is employed to describe these behaviours, with different functional forms of the fractional order introduced to reproduce the stress-strain response before and after the yield point. Model predictions are compared with the experimental results to evaluate performance and to demonstrate the advantages of the proposed VOF approach over conventional fractional order models.

### 3.1. Compression stress-strain response of PC at different temperatures

Fig. 5 presents the true stress-strain results from compression tests on PC conducted at a strain rate of 0.003 $s^{-1}$ at different temperatures. The experimental results of each loading condition correspond to the average response of at least three specimens. The error bars illustrate the graphical representations of the variability of data. The maximum deviation in the mechanical response remains below 10%. A pronounced reduction of the value in the true stress is observed with higher temperatures. The shape of the true stress-strain responses differs markedly below and above Tg, reflecting the transition from a glassy-dominated to rubbery deformation behaviour.

Fig. 5(a) shows the experimental data obtained below Tg at 60, 100, and 140 °C. At small strains, the stress increases linearly with strain, reflecting the elastic deformation of the polymer dominated by restricted molecular mobility. As deformation progresses, a distinct yield point is reached, followed by strain softening, which is commonly attributed to the initiation of localized molecular rearrangements. At larger strains, it exhibits strain hardening, as evidenced by the subsequent increase in true stress. This hardening behaviour is associated with progressive molecular chain orientation and stretching, which enhances resistance to further deformation despite the initially reduced stiffness after yielding.

Fig. 5(b) illustrates the mechanical behaviour of PC above Tg, at 160, 170, and 180 °C. Compared with the response below Tg, the true stress levels are markedly reduced, while a monotonic increase in true stress with true strain is observed. This behaviour is associated with the significant enhancement of molecular chain mobility in polymer above Tg, leading to a predominantly ductile, viscoelastic response. In this temperature range, the stress-strain curves no longer exhibit well-defined yield point and instead display smooth, strain-hardening behaviour. At 180 °C, the response is dominated by rubbery deformation mechanism, characterized by extensive chain segment mobility and reduced intermolecular resistance.

The stress-strain behaviour shows a transition between 140 and 160 °C, as the value of Tg lies within this temperature range. The polymer shifts from a rigid, glassy state to a more flexible, rubbery state. The evolution of true stress demonstrates strong temperature dependence and the stress values systematically decrease with increasing temperature.

Based on the pronounced differences in the stress-strain response below and above Tg, the numerical identification is performed separately with different constitutive models. This approach ensures that the constitutive behaviour laws are applied to describe the viscoelastic behaviours from glassy to rubbery states of PC.

### 3.2. Numerical identification of viscoelastic behaviour below Tg

The VOF model is proposed for describing the viscoelastic behaviour of PC below Tg. Different functions could be applied to the fractional order of the VOF models. A comparative analysis is carried out to determine the suitable function for the stress-strain responses below Tg. The parameters in the VOF models are characterized based on the experimental data by using LSM. The fitting accuracy is compared with that of the conventional fractional order models.

#### 3.2.1. Proposition of the fractional order function

The stress-strain curve of PC below Tg is presented in Fig. 6. It consists of an initial linear elastic region, and yielding up to the strengthening limit. After the yield point, it exhibits a strain softening and followed by the strain hardening. The mechanical behaviour before

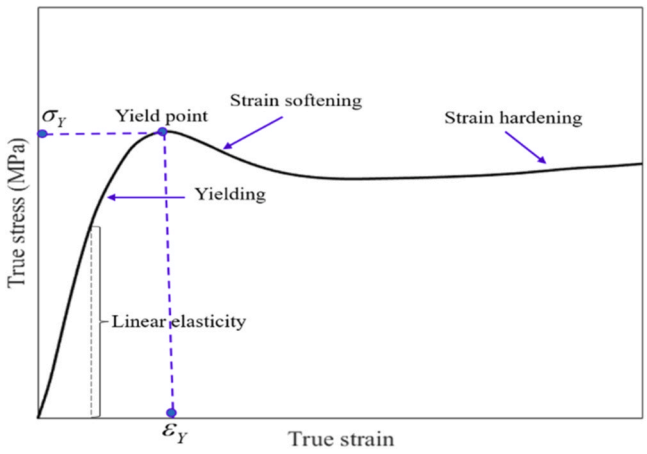


**Fig. 6.** Description of the experimental true stress-strain curve of PC under uniaxial compression below Tg (60, 100, or 140 °C).

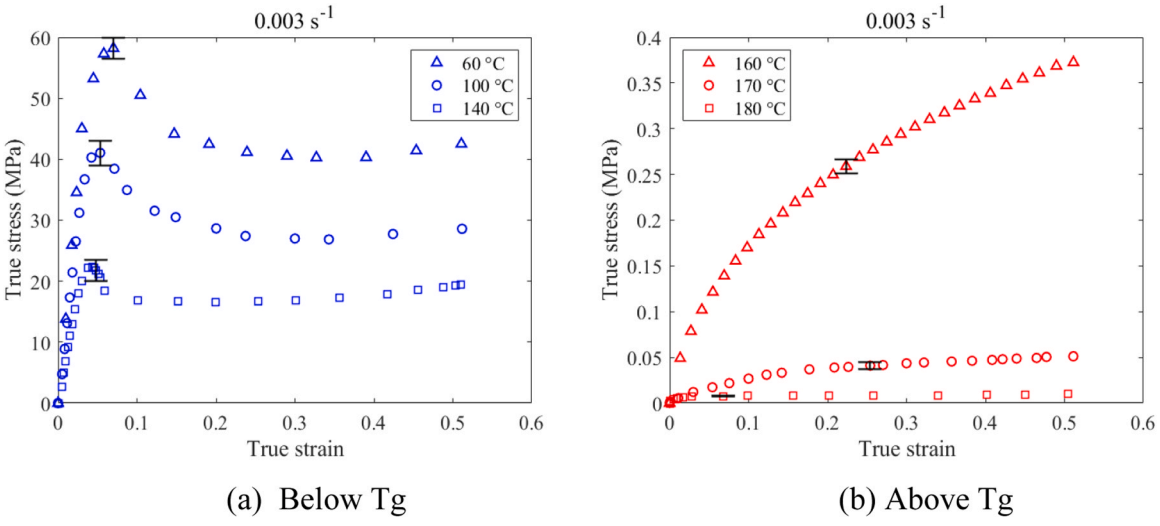


**Fig. 5.** True stress-strain responses at a strain rate of 0.003 $s^{-1}$ at different temperatures: (a) Below Tg, (b) Above Tg.

and after the yield point is different. The fractional order $\alpha(\varepsilon)$ is defined as a strain-dependent function to accurately describe the evolution of the stress-strain response.

The fractional order function is extended to a nonlinear function of strain to fit the stress-strain curve after the yield point. A power-law strain-dependent formulation is employed to characterize strain hardening and stress strengthening observed in the compression tests [29]. The fractional order in the VOF model below Tg is defined as given in Eq. (14), with the yield strain $\varepsilon_Y$ as a reference point.

$$\alpha_1(\varepsilon) = \begin{cases} a_1\varepsilon, & 0 \le \varepsilon \le \varepsilon_Y \\ c\varepsilon^d + e, & \varepsilon > \varepsilon_Y \end{cases} \tag{14}$$

where $a_1$ is the slope governing the linear strain dependence of the fractional order prior to yielding, $c$, $d$, and $e$ are the scaling, exponent, and offset parameters, respectively, characterizing the nonlinear evolution of the fractional order after yielding.

A parametric study is conducted to evaluate the efficiency of the power-law function $\alpha_1(\varepsilon) = c\varepsilon^d + e$ to describe large-deformation behaviour of PC. Based on the parameter identification performed on the experimental stress-strain responses, the elastic modulus and relaxation time in Eq. (10) are fixed at $E = 40$ MPa and $\theta = 400$ s, respectively, while the offset parameter is $e = 0.1$. Fig. 7 illustrates the influence of the parameters $c$ and $d$ on the predicted stress-strain response. The parameter ranges were chosen to ensure that the strain-dependent fractional order $\alpha(\varepsilon)$ remains between 0 and 1. In Fig. 7(a), the effect of the scaling parameter $c$ is investigated by fixing the exponent to $d = 1$ and varying $c$ over the range $\{0.1,\ 0.3,\ 0.5,\ 0.7\}$. This analysis highlights the $c$ influences on the magnitude of the strain-dependent fractional order. In Fig. 7(b), the influence of the power-law exponent $d$ is investigated by fixing $c = 0.5$ and considering four representative values $d = \{0.1,\ 0.5,\ 1,\ 2\}$. The exponent $d$ governs the nonlinear evolution of the fractional order with strain.

These results indicate that a linear order function is appropriate for describing the viscoelastic behaviour of PC under small strains, where the response remains nearly linear at temperatures below Tg, while a power-law fractional order function is required to accurately describe the large-deformation response.

Above Tg, a linear order function,

$$\alpha_2(\varepsilon) = a_2\varepsilon + b_2 \tag{15}$$

is adopted in VOF model to describe the mechanical behaviour observed in the rubbery regime. These formulations enable accurate identification of the VOF model across distinct thermo-mechanical regimes.

### 3.2.2. *Identification results below Tg*

The proposed order function as defined in Eq. (14) is employed in VOF model to describe the true stress-strain behaviour below Tg. As illustrated in Fig. 8, the model prediction and experimental data are consistent, confirming the accuracy of the proposed constitutive model.

The true strain is divided into pre-yield strain $\varepsilon_1$ and post-yield strain $\varepsilon_2$ to describe the different deformation mechanisms governing the response below Tg. As proposed the fractional order (Eq. (14)) is employed in VOF model prior to the yield point. This formulation is justified by the relatively small strains in this regime, where the nonlinearity of the mechanical response remains limited. Beyond the yield point, the order function adopts a power-law form, which ensures continuity at the yield point for each temperature and maintains physical consistency across the entire deformation range. The identified model parameters at different temperatures below Tg are summarized in Table 2.

The identified elastic modulus and relaxation time reflect the temperature-dependent viscoelastic behaviour of the material. Before yielding, $E_1$ represents the initial elastic modulus, which decreases progressively with temperature. The stiffness of the material decreases

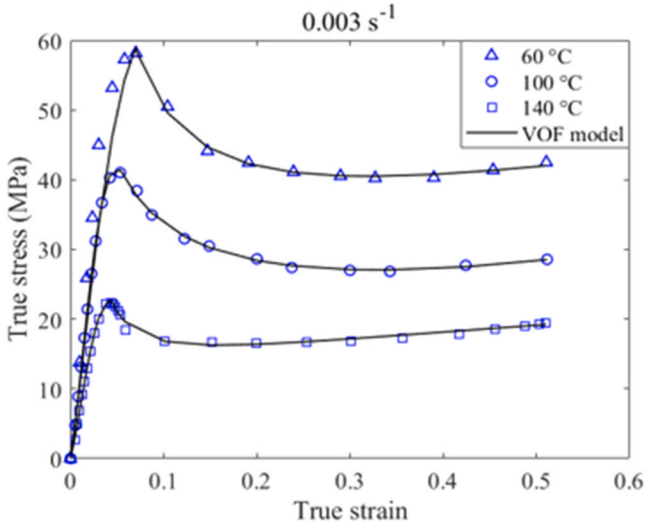


**Fig. 8.** Comparison between the experimental data and the VOF model predictions for the true stress-strain behaviour of PC at different temperatures below Tg.

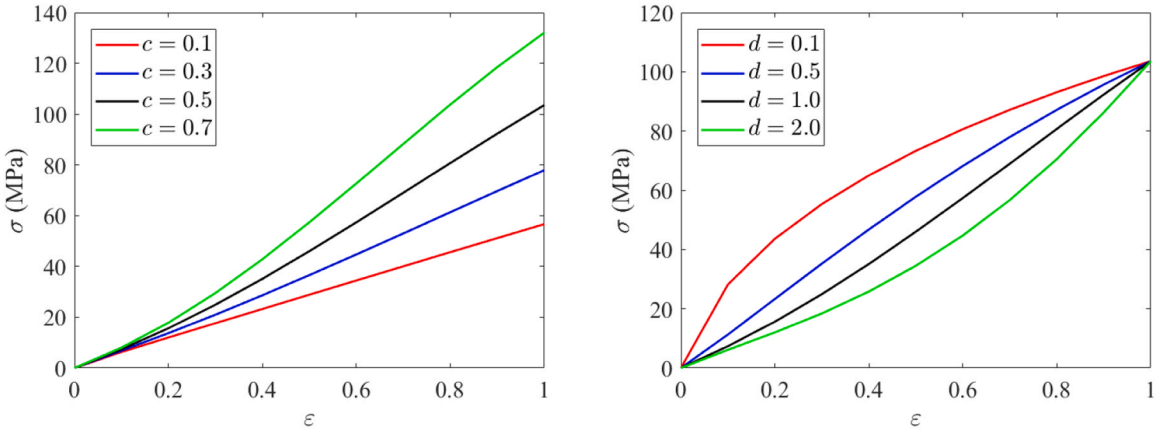


(a) $d = 1,\ c = \{0.1, 0.3, 0.5, 0.7\}$ (b) $c = 0.5,\ d = \{0.1, 0.5, 1.0, 2.0\}$

**Fig. 7.** Effects of the parameters (a) $c$ and (b) $d$ of the strain-dependent fractional order on stress-strain response.

**Table 2**
Identified VOF model parameters at different temperatures below Tg.

| $T$ (°C) | Before yielding | | | Yield strain | After yielding | | | | |
|---|---|---|---|---|---|---|---|---|---|
| | $a_1$ | $E_1$ (MPa) | $\theta_1$ (s) | $\varepsilon_Y$ | $c$ | $d$ | $e$ | $E_2$ (MPa) | $\theta_2$ (s) |
| 60 | 9 | 1346 | 9 | 0.07 | -1.86 | 0.66 | 1.31 | 72 | 268 |
| 100 | 16 | 820 | 14 | 0.05 | -1.38 | 0.56 | 1.23 | 40 | 370 |
| 140 | 19 | 493 | 15 | 0.04 | 0.10 | -0.45 | 0.51 | 12 | 853 |

with temperature near the glass transition regime. $\theta_1$, representing the relaxation time, increases with temperature and reflects the enhanced time-dependent viscous response [30]. After yielding, $E_2$ and $\theta_2$ exhibit a more pronounced temperature dependence. The substantial decrease in $E_2$ with temperature highlights the significant softening of the material in the post-yield regime [31]. The concurrent increase in $\theta_2$ indicates the dominant role of viscous flow and long-term relaxation processes as the polymer transitions into a more ductile state. This evolution of parameters with temperature and deformation underscores the capability of the VOF model to describe the complex thermo-mechanical behaviour of PC across a wide range of strain levels below Tg.

The evolution of the strain-dependent fractional order is illustrated in Fig. 9. It shows that at lower temperatures, the fractional order exhibits a rapid increase before yielding and a pronounced decrease after yielding due to the restricted molecular mobility. At higher temperatures, both the pre-yield increase and the post-yield decrease become more gradual, consistent with enhanced chain mobility and molecular rearrangement. The mechanical response before yielding corresponds to an elastic-dominated regime, described by a linear fractional order formulation. At the yield strain $\varepsilon_Y$, a distinct transition in the evolution law of the fractional order is introduced to capture the abrupt change in material behaviour. This transition represents the onset of irreversible molecular rearrangements and increased nonlinearity in the mechanical response. A discontinuity appears at the yield point, as shown in Fig. 9. Such a discontinuity is not a mathematical inconsistency but rather reflects a physical transition in the underlying deformation mechanism. Similar piecewise definitions have been adopted in the literature for VOF model to describe mechanical transitions of soft materials in [19]. Although the fractional order exhibits a jump at $\varepsilon_Y$, the stress response remains physically admissible, and no non-physical energy generation occurs. The fractional order remains within the admissible interval (0, 1), ensuring thermodynamic consistency of the model. These results demonstrate that the proposed VOF model describes the regime-dependent viscoelastic behavior of PC in the glassy state, including the transition at yielding.

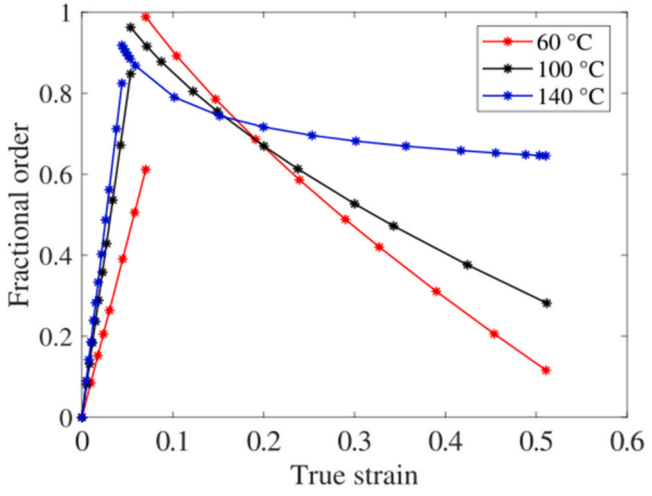


**Fig. 9.** Evolution of the fractional order as a function of true strain below Tg.

*3.2.3. Comparative analysis of the proposed VOF model and existing VOF models*

In contrast to the proposed approach of dividing the stress-strain curve into two regions based on the upper yield point, as shown in Fig. 10(a), Meng et al. [20] divided it into three regions using the upper and lower yield points ($\varepsilon_Y$ and $\varepsilon_{Y'}$), as illustrated in Fig. 10(b). Their VOF model contains three different order functions: a constant, a linear function, and another linear function for each region. It allows for detailed modelling of different deformation stages, but significantly increases the complexity of the parameter identification process due to the multiple order functions and additional transition boundaries. The present study proposes a simplified and effective formulation, avoiding multiple partitioning. The proposed VOF model is suitable to describe the essential nonlinear behaviour with fewer parameters, and improve both the efficiency and robustness of the parameter identification.

Fig. 11 compares experimental data on the true stress-strain response of PC at 60, 100, and 140 °C with these two VOF models. The proposed VOF model consistently aligns more closely with the experimental data, accurately describing both the pre-yield and post-yield regimes. The existing VOF model shows greater deviations near the yield point and at higher strains. This comparison underscores the capacity of the proposed model to account more effectively for temperature-dependent viscoelastic deformation in PC.

A quantitative comparison between the experimental true stress-strain responses and the corresponding simulations obtained using the proposed VOF model and the existing model reported in [20] is presented in Table 3. The fitting performance is evaluated in different deformation regions using the $R^2$ and the RMSE. The proposed VOF model consistently exhibits higher $R^2$ values and lower RMSE across all investigated temperatures, demonstrating an improved ability to reproduce the experimental response in both the pre-yield and post-yield regimes. In contrast, the model in [20] shows larger discrepancies, particularly in the vicinity of the yield point and at higher strain levels. These results highlight the superior capability of the proposed model to describe the temperature-dependent viscoelastic and inelastic deformation mechanisms governing the mechanical behaviour of PC below Tg.

Cai et al. [24] proposed a VOF model in which the fractional order was defined through three strain-dependent functions to describe the different deformation stages of polymers below Tg. In Region 1 (pre-yield regime), a linear strain-dependent fractional order was employed to describe the initial compressive response. In Region 2 (strain-softening stage), an increasing power-law evolution of the fractional order was introduced, replacing the linearly decreasing formulation adopted in [20]. This modification enhanced the model flexibility in representing the nonlinear softening behaviour. The re-hardening stage (Region 3) exhibits greater sensitivity to temperature compared with the viscoelastic and softening stages. The fractional order in [24] was formulated as an explicit temperature-dependent function in this regime.

The quantitative fitting results of the model in [24] for describing the true stress-strain responses of PC below Tg are summarized in Table 4. The VOF model in [24] significantly improves the fitting accuracy compared with results in Table 3, particularly in Regions 2 and 3. For example, at 60 °C, the value of $R^2$ exceeds 0.98 in all regions, while the RMSE values are substantially reduced compared with those reported for the model in [20], especially in the strain-softening stage.

The fitting efficiency of the proposed VOF model with the model in

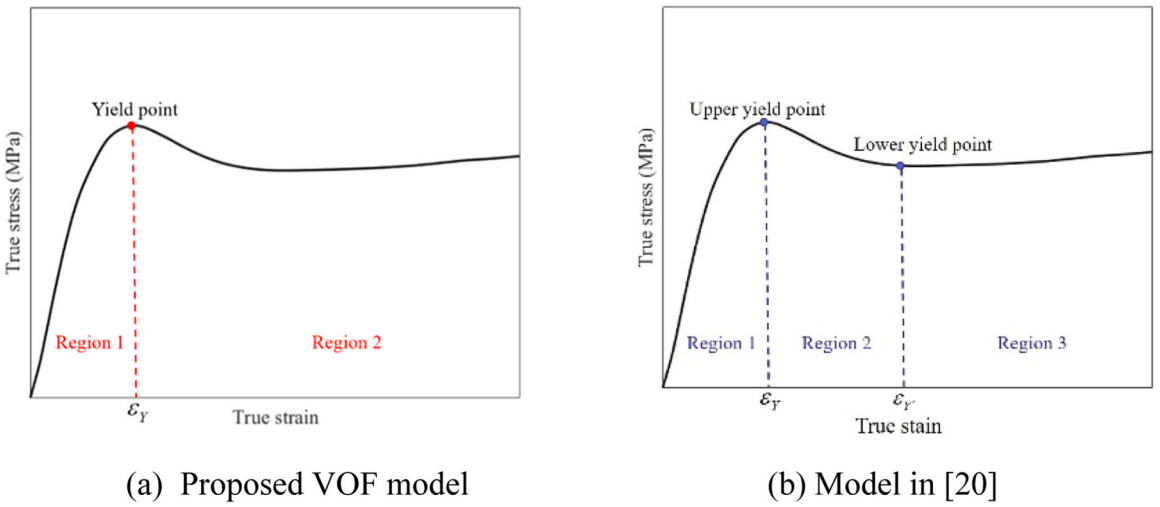


**Fig. 10.** Stress-strain curves below Tg: (a) Proposed VOF model, (b) Model in [20].

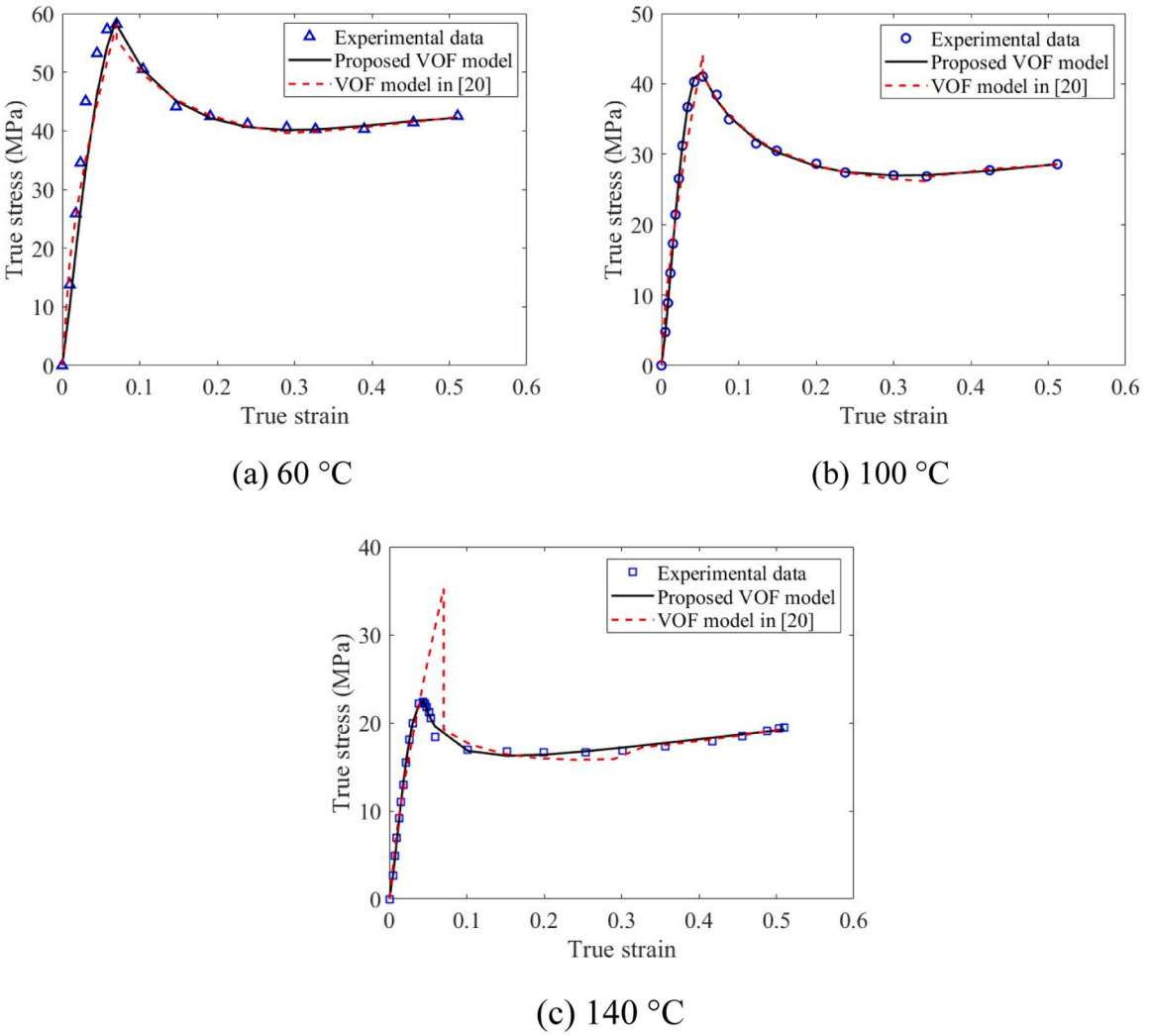


**Fig. 11.** Comparison between the experimental data and the simulation of the proposed VOF model and the existing model in [20] for the true stress-strain behaviour of PC below Tg: (a) 60 °C, (b) 100 °C, (c) 140 °C.

[24] is compared quantitatively in Tables 3 and 4, together with the fitting curves presented in Fig. 12. It shows that the proposed VOF model has a simple formulation and high fitting accuracy. The model in [24] requires multiple region-specific fractional order expressions and a larger number of adjustable parameters, which complicates the parameter identification procedure and may reduce model robustness. This

**Table 3**
Quantitative comparison of fitting accuracy between the proposed VOF model and model in [20] for PC below Tg.

| *T* (°C) | Proposed VOF model | | | | Model in [20] | | | | | |
|---|---|---|---|---|---|---|---|---|---|---|
| | Region 1 | | Region 2 | | Region 1 | | Region 2 | | Region 3 | |
| | $R^2$ | RMSE | $R^2$ | RMSE | $R^2$ | RMSE | $R^2$ | RMSE | $R^2$ | RMSE |
| 60 | 0.9985 | 0.34 | 0.9962 | 0.33 | 0.9267 | 5.43 | 0.9573 | 1.30 | 0.6162 | 0.53 |
| 100 | 0.9998 | 0.19 | 0.9948 | 0.33 | 0.9571 | 2.84 | 0.9904 | 0.48 | 0.9647 | 0.13 |
| 140 | 0.9997 | 0.12 | 0.9809 | 0.39 | 0.9702 | 1.26 | 0.8837 | 0.79 | 0.9733 | 0.18 |

**Table 4**
Quantitative results of fitting accuracy the existing model for PC below Tg.

| *T* (°C) | Model in [24] | | | | | |
|---|---|---|---|---|---|---|
| | Region 1 | | Region 2 | | Region 3 | |
| | $R^2$ | RMSE | $R^2$ | RMSE | $R^2$ | RMSE |
| 60 | 0.9985 | 0.334 | 0.9975 | 0.31 | 0.9820 | 0.12 |
| 100 | 0.9998 | 0.19 | 0.9945 | 0.36 | 0.9957 | 0.037 |
| 140 | 0.9997 | 0.12 | 0.9691 | 0.41 | 0.9988 | 0.037 |

model is formulated and validated exclusively for temperatures below Tg, which limits its applicability to broader thermo-mechanical conditions. The proposed VOF model seeks to maintain high fitting accuracy using a more compact parameter set and a unified formulation across different deformation stages, thereby improving both computational efficiency and generalization capability.

### 3.3. Numerical identification of viscoelastic behaviour above Tg

A VOF model with a strain-dependent linear order function Eq. (15) is employed to characterize the viscoelastic behaviour of PC above Tg. The model parameters are identified from the experimental data. The predictive performance of the proposed VOF model is evaluated by comparing the results with both experimental observations and COF model simulations. This confirms the strong capability of the VOF model to describe the nonlinear viscoelastic behaviour over a wide strain range.

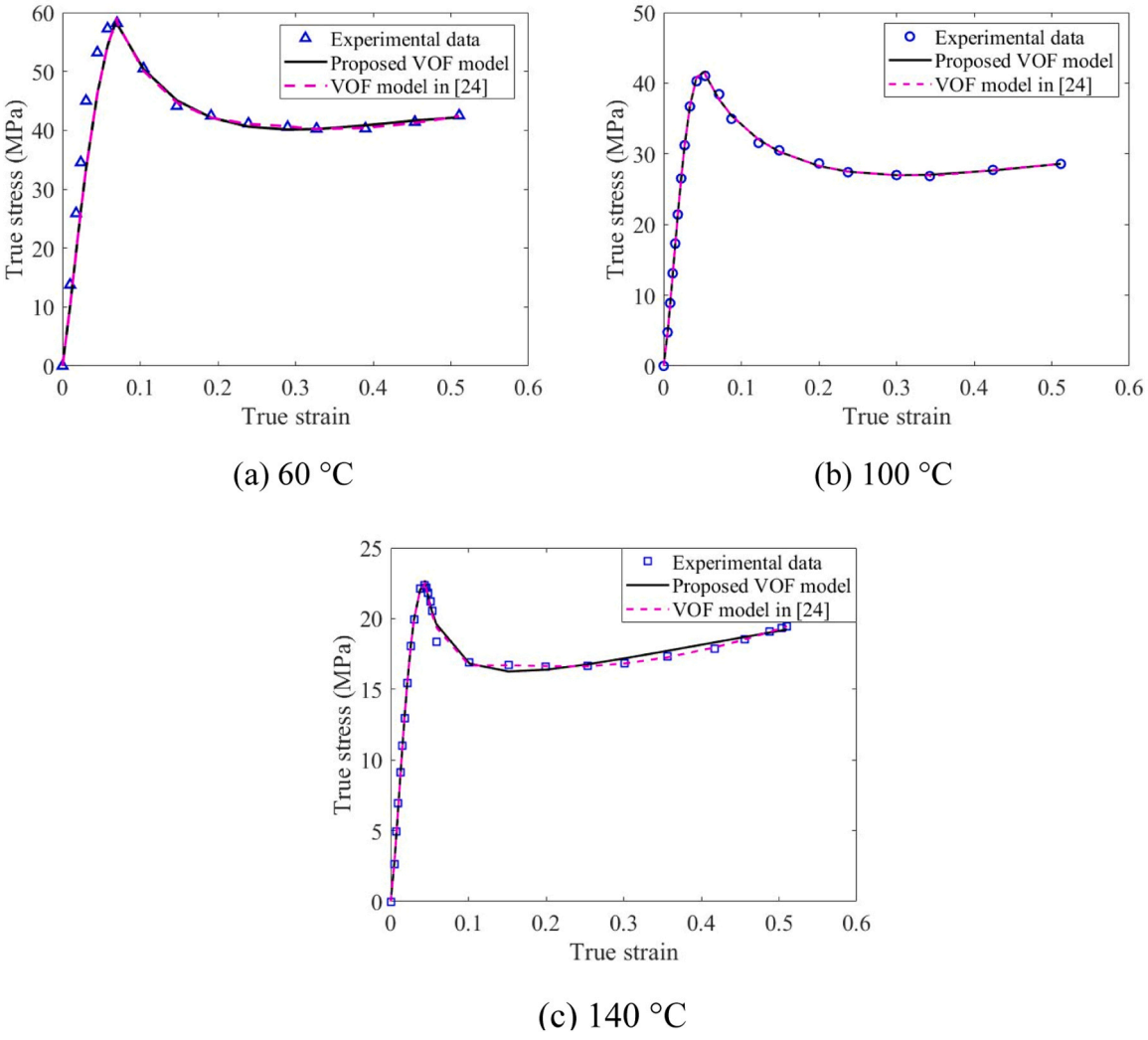


**Fig. 12.** Comparison between the experimental data and the simulation of the proposed VOF model and the existing model in [24] for the true stress-strain behaviour of PC below Tg: (a) 60 °C, (b) 100 °C, (c) 140 °C.

### 3.3.1. Identification results above Tg

The fitting results presented in Fig. 13 demonstrate good agreement between the VOF model predictions and the experimental data for temperatures above Tg (160, 170, and 180 °C).

The identified parameters and quantitative metrics of the VOF model are summarized in Table 5. The high $R^2$ values obtained at all investigated temperatures indicate an excellent agreement between the VOF model predictions and the experimental data. The consistently low RMSE values further confirm the robustness and accuracy of the proposed VOF model in describing the viscoelastic response of PC above Tg.

These results show that the elastic modulus $E$ decreases with temperature due to the scission of the macromolecular chains. The relaxation time $\theta$ increases with temperature. It reflects the extended timescales associated with molecular relaxation processes in the highly softened state. At elevated temperatures, polymer chains experience enhanced segmental mobility and slippage. It allows the stress relaxation to occur over a longer period.

As illustrated in Fig. 14, the fractional order increases gradually with temperature, indicating enhanced molecular mobility and a more pronounced time-dependent viscoelastic response at elevated thermal temperatures.

### 3.3.2. Comparative analysis of the proposed VOF model and COF model

The numerical predictions of the true stress-strain curve with the COF model defined in Eq. (3) and the proposed VOF model are compared, as shown in Fig. 15. The results demonstrate that the VOF model provides a more accurate description of the mechanical behaviour, especially at larger strains.

Table 6 highlights the identified parameters of the COF model for PC at different temperatures above Tg, together with the corresponding correlation parameters $R^2$ and RMSE. The identified parameters exhibit similar trends to those obtained with the VOF model. The fractional order $\alpha$ increases monotonically with temperature, indicating a gradual transition toward a more fluid-like viscoelastic response.

A quantitative comparison between the results obtained with the COF model (Table 6) and the VOF model (Table 5) is performed using the fitting metrics. The VOF model consistently yields lower RMSE values and higher $R^2$. This demonstrates that the constant fractional order limits the ability of the COF model to describe the nonlinear viscoelastic response in the rubbery regime, where strain-dependent effects become significant.

The proposed VOF framework preserves a unified constitutive structure and modelling philosophy across both glassy and rubbery regimes. The existing fractional order models, although demonstrating good accuracy when applied either below or above Tg, generally rely on regime-specific formulations and parameter sets. The present approach enables a consistent and continuous interpretation of viscoelastic behaviour across Tg under different temperatures.

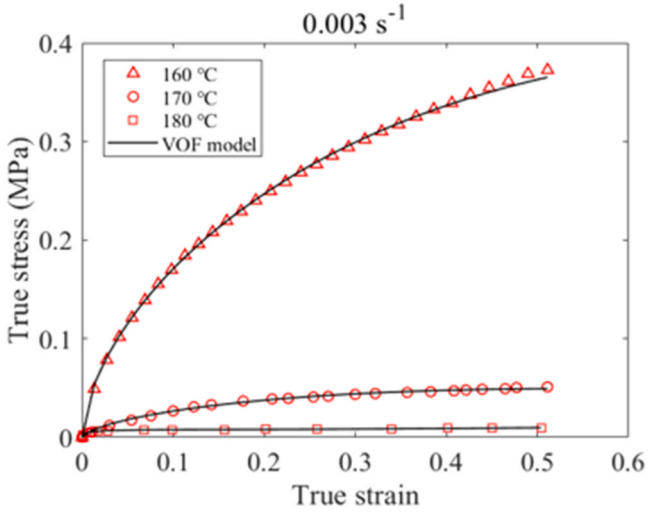


**Fig. 13.** Comparison between the experimental data and the VOF model predictions for the true stress-strain behaviour of PC above Tg.

**Table 5**
Identified parameters of the VOF model at temperatures above Tg.

| $T$ (°C) | $a$ | $b$ | $E$ (MPa) | $\theta$ (s) | $R^2$ | RMSE |
|---|---|---|---|---|---|---|
| 160 | 0.1780 | 0.361 | 2.412 | 9.120 | 0.9998 | $3.40 \times 10^{-3}$ |
| 170 | 0.275 | 0.383 | 0.401 | 9.330 | 0.9988 | $1.01 \times 10^{-3}$ |
| 180 | 0.001 | 0.877 | 0.179 | 16.338 | 0.9995 | $9.62 \times 10^{-5}$ |

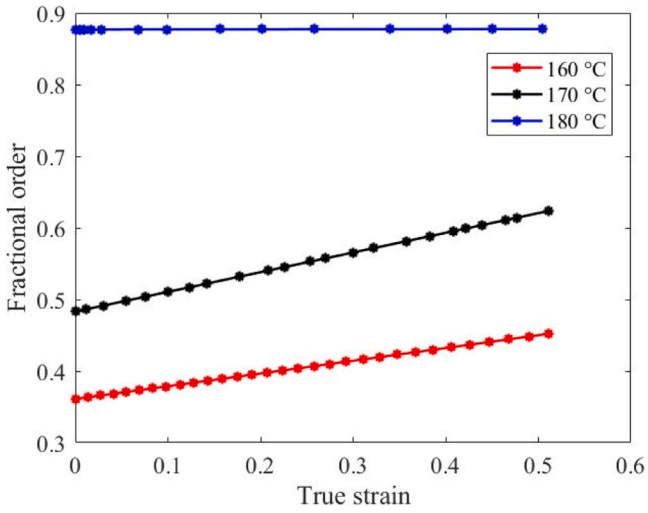


**Fig. 14.** Evolution of the fractional order as a function of true strain above Tg.

## 4. Discussion and model assessment

This section provides a general discussion and assessment of the proposed VOF model. The thermodynamic admissibility of the formulation is examined to ensure its physical consistency. The applicability of the proposed framework to other amorphous polymers is discussed. The model's capability in describing loading-unloading responses and irreversible deformation mechanisms are addressed.

### 4.1. Thermodynamic considerations of the VOF model

The thermodynamic consistency of COF viscoelastic models was well established as reported in [32]. When the fractional order is constant and all material parameters are strictly positive, such models satisfy the second law of thermodynamics and exhibit physically admissible creep and relaxation responses. Thermodynamic constraints requiring non-negative energy dissipation ensure a physically meaningful description of viscoelastic behaviours [33].

The thermodynamic consistency for VOF models should be carefully assessed. It depends on both the definition of the fractional operator and the fractional order function. In the present work, the proposed VOF formulation (Eq. (10)) is not derived from a variational framework built on an explicit Helmholtz free energy and a complementary dissipation potential [34]. The thermodynamic admissibility is ensured by imposing physically motivated constraints on the model parameters, derived from the requirement of non-negative storage and loss moduli in the steady-state regime [35].

All material parameters in the proposed VOF model are constrained to be strictly positive, and the strain-dependent fractional order is required to satisfy $0 < \alpha(\varepsilon) < 1$, as illustrated in Fig. 9 and Fig. 14.

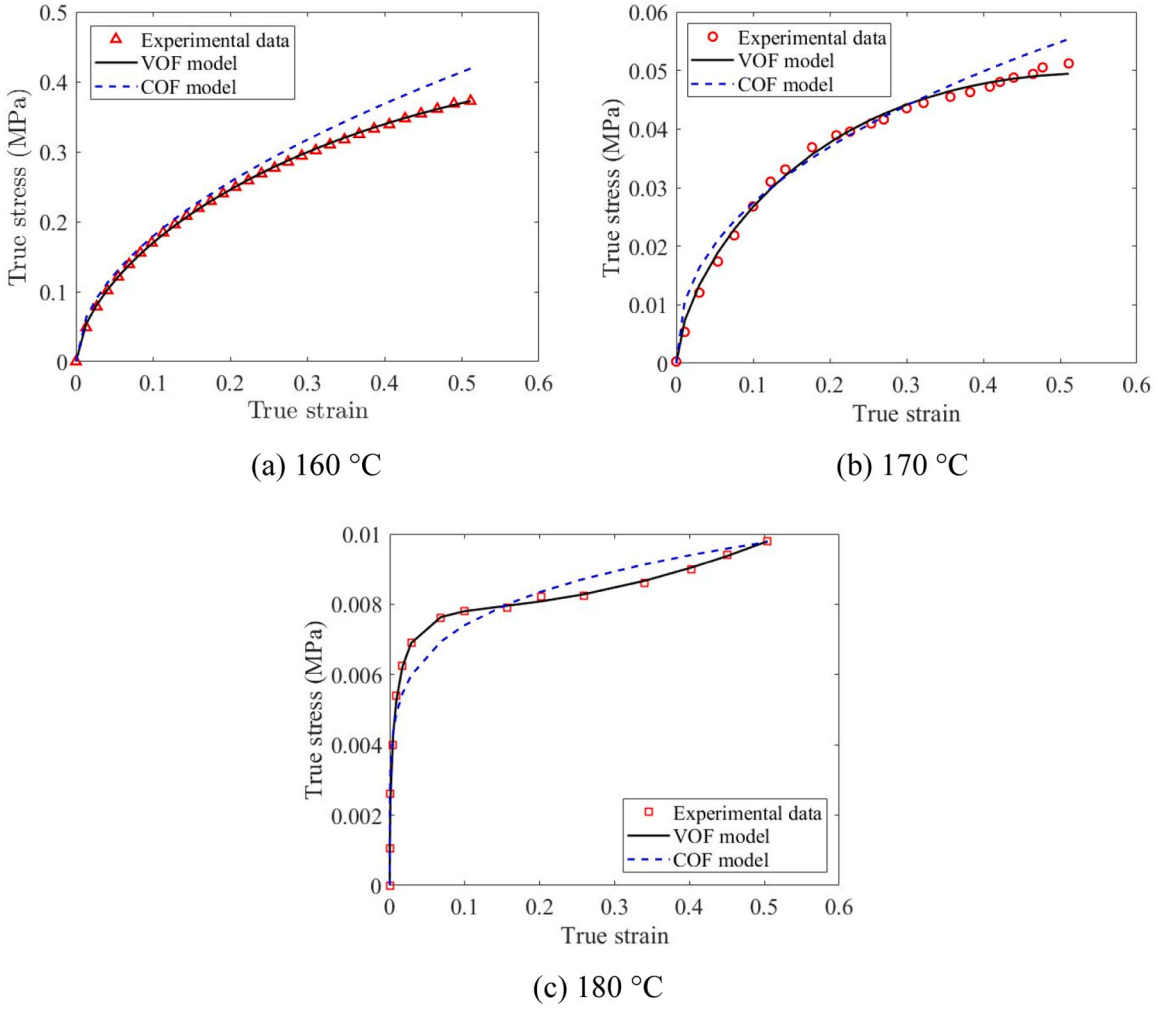


**Fig. 15.** Comparison between the experimental data and the simulations of the COF and VOF models for the true stress-strain behaviour of PC above Tg: (a) 160 °C, (b) 170 °C, and (c) 180 °C.

**Table 6**
Identified parameters of the COF model at temperatures above Tg.

| $T$ (°C) | $\alpha$ | $E$ (MPa) | $\theta$ (s) | $R^2$ | RMSE |
|---|---|---|---|---|---|
| 160 | 0.48 | 3.80 | 1.32 | 0.9510 | $2.19 \times 10^{-2}$ |
| 170 | 0.57 | 1.52 | 3.89 | 0.9683 | $2.60 \times 10^{-3}$ |
| 180 | 0.83 | 0.41 | 5.43 | 0.9602 | $5.80 \times 10^{-4}$ |

Under these conditions, the model can be locally interpreted as a Scott-Blair fractional viscoelastic element, which is passive and dissipative under isothermal loading. Consequently, no non-physical energy generation occurs during deformation.

The thermodynamic consistency of the proposed model is examined under isothermal small-strain conditions. Under these assumptions, the local form of the Clausius-Duhem inequality reduces to the mechanical dissipation inequality:

$$\mathscr{D}(t) = \sigma(t)\dot{\varepsilon}(t) - \dot{\psi}(t) \geq 0 \tag{16}$$

where $\psi$ denotes the Helmholtz free-energy density.

For a given instantaneous value of the strain-dependent order $\alpha(\varepsilon)$, the VOF model locally coincides with a Scott-Blair fractional element. In one-dimension, the constitutive behaviour law is written as:

$$\sigma(t) = E\theta^{\alpha(\varepsilon)} D_t^{\alpha(\varepsilon)} \varepsilon(t) \tag{17}$$

where $E > 0$, $\theta > 0$, and $0 < \alpha(\varepsilon) < 1$.

According to the theory of the Grünwald-Letnikov (GL) VOF derivative, the VOF operator of $f(t)$ is defined as [36]:

$$D_t^{\alpha(t)} f(t) = \lim_{h \to 0^+} h^{-\alpha(t)} \sum_{k=0}^{\infty} \frac{(-\alpha(t))_k}{k!} f(t - kh) \tag{18}$$

where $f(t)$, $t \in \mathbb{R}$, is any function, $h$ denotes a positive time increment, $k = 0, 1, 2, \ldots$, and $(-\alpha(t))_k$ is Pochhammer symbol.

A fundamental property of this definition is that exponential functions remain eigenfunctions of the operator. In particular, for $f(t) = e^{st}$, $s \in \mathbb{C}$, and $\mathrm{Re}(s) > 0$,

$$D_t^{\alpha(t)} e^{st} = s^{\alpha(t)} e^{st} \tag{19}$$

As a consequence, for harmonic functions $f(t) = e^{i\omega t}$,

$$D_t^{\alpha(t)} e^{i\omega t} = (i\omega)^{\alpha(t)} e^{i\omega t} \tag{20}$$

which implies that

$$D_t^{\alpha(t)} \cos(\omega t) = (\omega)^{\alpha(t)} \cos\left(\omega t + \frac{\pi}{2}\alpha(t)\right) \tag{21}$$

In the GL framework, complex exponentials remain eigenfunctions even when the order varies with time.

If the functions admit a Laplace transform, the VOF derivative can be expressed via the Bromwich inversion integral:

$$D_t^{\alpha(t)} f(t) = \frac{1}{2\pi i} \int_{\beta-i\infty}^{\beta+i\infty} s^{\alpha(t)} F(s) e^{st} ds \tag{22}$$

where $F(s)$ is the Laplace transform of $f(t)$, and the integration contour $\mathrm{Re}(s) = \beta$ lies within the region of convergence of $F(s)$.

This representation provides the theoretical foundation for the spectral characterization of the operator. Under vanishing initial conditions and steady-state harmonic loading, the Fourier transform $\mathscr{F}$ corresponds to evaluating the Laplace transform along the imaginary axis ($s = i\omega$), yielding:

$$\mathscr{F}\left[D_t^{\alpha(\varepsilon)} \varepsilon(t)\right] = (i\omega)^{\alpha(\varepsilon)} \mathscr{F}[\varepsilon(t)] \tag{23}$$

In the framework of the forward GL definition and for functions admitting a Laplace transform, the operator admits a frequency-domain symbol $s^{\alpha(t)}$, which justifies the transition from time to frequency domain adopted in the present work.

Applying this property to proposed model in Eq. (17) leads to the strain-dependent complex modulus:

$$E^*(\omega, \quad \varepsilon) = E(i\omega\theta)^{\alpha(\varepsilon)} \tag{24}$$

Using the principal-branch representation:

$$(i\omega\theta)^{\alpha(\varepsilon)} = (\omega\theta)^{\alpha(\varepsilon)} e^{i\alpha(\varepsilon)\pi/2} = (\omega\theta)^{\alpha(\varepsilon)} \left[\cos\left(\frac{\pi\alpha(\varepsilon)}{2}\right) + i\sin\left(\frac{\pi\alpha(\varepsilon)}{2}\right)\right] \tag{25}$$

in which the storage and loss moduli are obtained as:

$$E'(\omega, \varepsilon) = E(\omega\theta)^{\alpha(\varepsilon)} \cos\left(\frac{\pi\alpha(\varepsilon)}{2}\right) \tag{26}$$

$$E''(\omega, \varepsilon) = E(\omega\theta)^{\alpha(\varepsilon)} \sin\left(\frac{\pi\alpha(\varepsilon)}{2}\right) \tag{27}$$

where both $E'(\omega, \varepsilon)$ and $E''(\omega, \varepsilon)$ are strictly non-negative with $E > 0$, $\theta > 0$, $0 < \alpha(\varepsilon) < 1$, and $\omega > 0$. The dissipated energy is positive, ensuring passivity of the constitutive operator and compliance with the Clausius-Duhem inequality.

The above derivation shows that, within the forward GL framework and for functions admitting a Laplace transform, the VOF derivative possesses a well-defined spectral representation through the symbol $s^{\alpha(t)}$. This provides the theoretical justification for the frequency-domain formulation adopted in Eqs. (24-27). A fully nonlinear thermodynamic formulation based on an explicit Helmholtz free-energy functional and an associated dissipation potential remains an open extension for future work.

### 4.2. General applicability of the proposed VOF model

The proposed VOF model is employed to describe the strain-dependent viscoelastic properties of amorphous thermoplastic polymers. The fractional order is defined as an internal variable that can be expressed as a function of strain, temperature, or strain rate. This flexibility makes the proposed framework applicable to other amorphous polymers exhibiting strong thermo-viscoelastic and nonlinear deformation behaviours, such as poly(methyl methacrylate), polyethylene terephthalate, or polystyrene. Future work will explore the efficiency of the proposed VOF model for other polymers under various loading conditions and temperature ranges.

### 4.3. Loading-unloading response in PC

The experimental results in this work are based on monotonic uniaxial compression tests. When unloading is considered, amorphous polymers possess recoverable elastic strain and irreversible plastic deformation, resulting in residual strain and mechanical hysteresis. Loading-unloading tests were performed on PC at 140 °C with a strain rate of 0.001 $s^{-1}$ . Fig. 16 presents the corresponding true stress-strain curve with 8% experimental uncertainty indicated by the error bar. The true strain recovers partially to 0.4881 after unloading, which confirms the time-dependent viscoelastic recovery and permanent deformation.

Fractional order models have been employed to describe the stress-strain responses under loading-unloading conditions. The study in [37] demonstrated that fractional order formulations can accurately characterize rate-dependent viscoelastic behaviours of polymers. These models have been developed to describe mean stress evolution and ratcheting strain in polymeric materials subjected to cyclic loading, providing effective representations of experimental observations over multiple cycles [38]. The VOF models have been extended to describe unloading behaviour. The fractional order function at different unloading strains was obtained by shifting the order function defined at a reference strain, and the feasibility of this approach was validated based on the comparisons with experimental data [39].

Despite these advances in the literature, several limitations remain. First, most existing models treat loading and unloading processes separately or require different functional forms of the fractional order for distinct stages, which increases the number of model parameters and limits predictive generality. Second, the evolution of the fractional order during cyclic loading is often prescribed phenomenologically, without fully capturing the continuous interaction between loading and unloading within a unified framework. Third, the extension of VOF models to fully cyclic processes, including hysteresis evolution and stiffness degradation, remains insufficiently explored.

In light of these limitations, further research is required to explore a unified VOF framework capable of describing the entire loading-unloading cycle as a continuous process. Such an approach would involve redefining the functional form of the strain-dependent fractional order so that both loading and unloading behaviours are described within one consistent evolution law. This enables a reduction in the number of model parameters while improving predictive robustness. The extension of the VOF formulation to cyclic loading conditions could provide deeper insight into hysteresis evolution, memory effects, and progressive material degradation, thereby broadening the applicability of VOF models in polymer mechanics.

## 5. Conclusions and perspectives

In this study, a VOF model is proposed to describe the viscoelastic behaviour of amorphous thermoplastic PC across a wide temperature range (below and above Tg). Experimental data obtained by

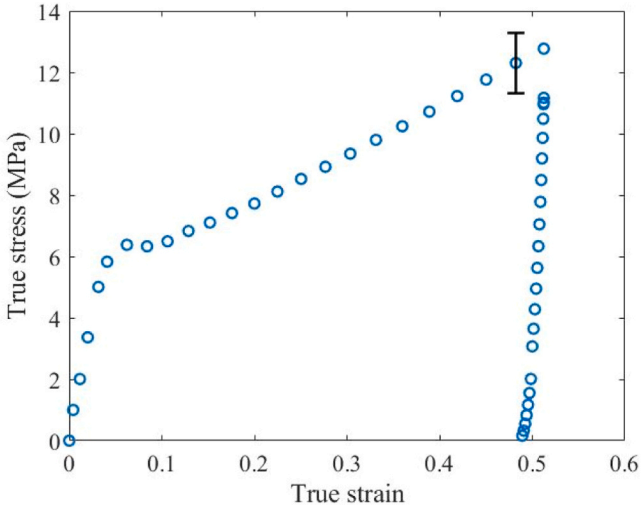


**Fig. 16.** Experimental loading-unloading true stress-strain response of PC with a strain rate of 0.001 $s^{-1}$ at 140 °C.

compression tests are used to identify the material parameters. A comparative analysis with the existing VOF and COF models is carried out. The main conclusions are as follows:

1. The proposed VOF model with less parameters effectively describes the viscoelastic properties of PC at different temperatures.
2. Various strain-dependent functions have been proposed for the fractional order based on the shape of the stress-strain curves. Above Tg, a linear order function is suitable. Below Tg, a combination of linear and power-law order functions is required for higher accuracy.
3. Compared to other COF and VOF models, the proposed VOF model exhibits greater accuracy with fewer identified parameters.
4. The thermodynamic admissibility of the proposed VOF model was examined and confirmed based on the physically motivated model parameters and the boundedness of the fractional order.

The proposed VOF model can be extended to describe complex nonlinear viscoelastic behaviour of other amorphous polymers. Its efficiency and accuracy will be investigated under more complex loading conditions, including loading-unloading and cyclic responses with irreversible deformation and hysteresis effects.

## CRediT authorship contribution statement

**Lin Sun:** Investigation, Writing – original draft, Software, Data curation, Validation. **Gang Cheng:** Supervision, Writing – review & editing. **Thierry Barrière:** Supervision, Writing – review & editing.

## Declaration of Competing Interest

The authors declare that they have no known competing financial interests or personal relationships that could have appeared to influence the work reported in this paper.

## Acknowledgments

This work is supported by China Scholarship Council (No. 2022018130033). The authors would like to thank the MIFHYSTO and AMETISTE platforms of the Applied Mechanics Department of the FEMTO-ST Institute for access to experimental facilities.

## Data availability

Data will be made available on request.

## References

[1] Z. Liang, J. Li, X. Zhang, Q. Kan, A viscoelastic-viscoplastic constitutive model and its finite element implementation of amorphous polymers, Polym. Test. 114 (2022) 107831, https://doi.org/10.1016/j.polymertesting.2022.107831.
[2] F.K. Aldawood, Multi-criteria optimization of polymer selection for biomedical additive manufacturing using analytic hierarchy process, Mater. Des. 256 (2025) 114369, https://doi.org/10.1016/j.matdes.2025.114369.
[3] S. Eshkalak, E. Ghomi, Y. Dai, D. Choudhury, S. Ramakrishna, The role of three-dimensional printing in healthcare and medicine, Mater. Des. 194 (2020) 108940, https://doi.org/10.1016/j.matdes.2020.108940.
[4] S. Mirkhalaf, F. Pires, An elasto-viscoplastic constitutive model for polymers at finite strains: formulation and computational aspects, Comput. Struct. 166 (2016) 60–74, https://doi.org/10.1016/j.compstruc.2016.01.002.
[5] R. Xiao, H. Sun, W. Chen, A finite deformation fractional viscoplastic model for the glass transition behavior of amorphous polymers, Int. J. Nonlin. Mech. 93 (2017) 7–14, https://doi.org/10.1016/j.ijnonlinmec.2017.04.019.
[6] W. Cai, Z. Wang, F. Wang, Temperature and strain-rate dependent fractional constitutive model for glassy polymers, Chaos Solitons Fract. 185 (2024) 115116, https://doi.org/10.1016/j.chaos.2024.115116.
[7] F. Luo, X. Liu, C. Shao, J. Zhang, C. Shen, Z. Guo, Micromechanical analysis of molecular orientation in high-temperature creep of polycarbonate, Mater. Des. 144 (2018) 25–31, https://doi.org/10.1016/j.matdes.2018.02.025.
[8] A. Alves, B. Ferreira, F. Pires, Constitutive modeling of amorphous thermoplastics from low to high strain rates: formulation and critical comparison employing an optimization-based parameter identification, Int. J. Solids Struct. 273 (2023) 112258, https://doi.org/10.1016/j.ijsolstr.2023.112258.
[9] A. Alves, B. Ferreira, F. Pires, A constitutive model for amorphous thermoplastics from low to high strain rates: formulation and computational aspects, Int. J. Plast. 169 (2023) 103712, https://doi.org/10.1016/j.ijplas.2023.103712.
[10] V. Gopalakrishnan, R. Pramanik, A. Arockiarajan, Unified rheological modeling using fractal calculus for soft biological matter, Mater. Des. 258 (2025) 114572, https://doi.org/10.1016/j.matdes.2025.114572.
[11] B. Zeng, Existence for a class of time-fractional evolutionary equations with applications involving weakly continuous operator, Fract. Calc. Appl. Anal. 26 (2023) 172–192, https://doi.org/10.1007/s13540-022-00125-0.
[12] R. Pramanik, F. Soni, K. Shanmuganathan, A. Arockiarajan, Mechanics of soft polymeric materials using a fractal viscoelastic model, Mech. TimeDepend. Mater. 26 (2022) 257–270, https://doi.org/10.1007/s11043-021-09486-0.
[13] R. Pramanik, A. Narayanan, A. Rajan, S. Konar, A. Arockiarajan, Transversely isotropic freeze-dried PVA hydrogels: theoretical modelling and experimental characterization, Int. J. Eng. Sci. 144 (2019) 103144, https://doi.org/10.1016/j.ijengsci.2019.103144.
[14] A. Salazar-Martín, M. Pérez, A. García-Granada, G. Reyes, J. Puigoriol-Forcada, A study of creep in polycarbonate fused deposition modelling parts, Mater. Des. 141 (2018) 414–425, https://doi.org/10.1016/j.matdes.2018.01.008.
[15] B. Han, D. Yin, Y. Gao, Analysis of the variable-order fractional viscoelastic modeling with application to polymer materials, Polym. Adv. Technol. 34 (2023) 2707–2720, https://doi.org/10.1002/pat.6084.
[16] L. Ramirez, C. Coimbra, A variable order constitutive relation for viscoelasticity, Ann. Phys. 16 (2007) 522–543, https://doi.org/10.1002/andp.200710246.
[17] Y. Gao, B. Zhao, M. Tang, D. Yin, Fractional modelling of salinity/temperature-dependent shear rheological behavior including stress overshoot for bentonite clay suspensions, Appl. Math. Model. 120 (2023) 267–280, https://doi.org/10.1016/j.apm.2023.04.004.
[18] Y. Gao, Y. Yang, F. Ren, B. Han, Variable-order fractional approach for modeling viscoelastic-plastic deformation in multistage compressive response of polymer syntactic foams, Commun. Nonlinear Sci. Numer. 149 (2025) 108915, https://doi.org/10.1016/j.cnsns.2025.108915.
[19] Y. Gao, D. Yin, B. Zhao, A variable-order fractional constitutive model to characterize the rate-dependent mechanical behavior of solid materials, Fractal Fract. 6 (2022) 590, https://doi.org/10.3390/fractalfract6100590.
[20] R. Meng, D. Yin, S. Lu, G. Xiang, Variable-order fractional constitutive model for the time-dependent mechanical behavior of polymers across the glass transition region, Eur. Phys. J. 134 (2019) 376, https://doi.org/10.1140/epjp/i2019-12767-x.
[21] G. Xiang, D. Yin, R. Meng, C. Cao, Predictive model for stress relaxation behavior of glassy polymers based on variable-order fractional calculus, Polym. Adv. Technol. 32 (2021) 703–713, https://doi.org/10.1002/pat.5123.
[22] W. Cai, P. Wang, Rate-dependent fractional constitutive model for nonlinear behaviors of rubber polymers, Eur. J. Mech. A Solids 103 (2024) 105186, https://doi.org/10.1016/j.euromechsol.2023.105186.
[23] W. Cai, Z. Wang, Y. Zhang, C. Liu, Microbiology-inspired nonlinear variable-order fractional model for amorphous glassy polymer, Acta Mech. 235 (2024) 7027–7038, https://doi.org/10.1007/s00707-024-04089-5.
[24] W. Cai, P. Wang, Fractional modeling of temperature-dependent mechanical behaviors for glassy polymers, Int. J. Mech. Sci. 232 (2022) 107607, https://doi.org/10.1016/j.ijmecsci.2022.107607.
[25] P. van Ekeren, C. Holl, A. Witteveen, A comparative test of differential scanning calorimeters, J. Therm. Anal. 49 (1997) 1105–1114, https://doi.org/10.1007/BF01996799.
[26] N. Heymans, Fractional calculus description of non-linear viscoelastic behaviour of polymers, Nonlinear Dynam 38 (2004) 221–231, https://doi.org/10.1007/s11071-004-3757-5.
[27] S. Majumdar, S. Hazra, M. Choudhury, S. Sinha, S. Das, T. Middya, S. Tarafdar, T. Dutta, A study of the rheological properties of visco-elastic materials using fractional calculus, Colloids Surf. A Physicochem. Eng. Asp. 516 (2017) 181–189, https://doi.org/10.1016/j.colsurfa.2016.12.019.
[28] W. Smit, H. Vries, Rheological models containing fractional derivatives, Rheol. Acta 9 (1970) 525–534, https://doi.org/10.1007/BF01985463.
[29] C. Wei, P. Wang, H. Zhang, Y. Wang, Linking fractional model to power-law constitutive model with applications to nonlinear polymeric stress-strain responses, Mech. TimeDepend. Mater. 27 (2022) 875–888, https://doi.org/10.1007/s11043-022-09558-9.
[30] A. Drozdov, J. Christiansen, Modeling the non-isothermal viscoelastic response of glassy polymers, Acta Mech. 229 (2018) 1137–1156, https://doi.org/10.1007/s00707-017-2053-7.
[31] A. Drozdov, Effect of yielding on the viscoelastic response of amorphous glassy polymers, J. Appl. Polym. Sci. 80 (2001) 2383–2393, https://doi.org/10.1002/app.1345.
[32] T. Atanackovic, S. Konjik, L. Oparnica, D. Zorica, Thermodynamical restrictions and wave propagation for a class of fractional order viscoelastic rods, Abstr. Appl. Anal. 2011 (2011) 32, https://doi.org/10.1155/2011/975694.
[33] T. Atanackovica, M. Janev, S. Pilipovic, Restrictions in a distributed complex fractional order linear constitutive equation of viscoelasticity, Phys. D. 456 (2023) 133917, https://doi.org/10.1016/j.physd.2023.133917.
[34] A. Narayanan, A. Rajan, R. Pramanik, A. Arockiarajan, A thermodynamically-consistent phenomenological viscoplastic model for hydrogels, Mater. Res. Express 6 (2019) 085418, https://doi.org/10.1088/2053-1591/ab2a49.
[35] R. Bagley, P. Torvik, On the fractional calculus model of viscoelastic behavior, J. Rheol. 30 (1986) 133, https://doi.org/10.1122/1.549887.

[36] M. Ortigueira, D. Valério, J. Machado, Variable order fractional systems, Commun. Nonlinear Sci. Numer. Simula 71 (2019) 231–243, https://doi.org/10.1016/j.cnsns.2018.12.003.
[37] Y. Gao, D. Yin, B. Zhao, Fractional description for the rate-dependent viscoelastic response of tough hydrogels, Polym. Adv. Technol. 33 (2022) 2708–2719, https://doi.org/10.1002/pat.5726.
[38] W. Cai, Y. Zhang, P. Wang, Z. Wang, Fractional modeling of cyclic loading behavior of polymeric materials, Mech. TimeDepend. Mater. 28 (2024) 1743–1759, https://doi.org/10.1007/s11043-024-09705-4.
[39] L. Wu, W. Cai, Z. Wang, J. Wang, A novel variable fractional constitutive model for complex multistage polymeric behaviors, Int. J. NonLinear Mech. 180 (2026) 105255, https://doi.org/10.1016/j.ijnonlinmec.2025.105255.